AIAA AVIATION Forum
12-16 June 2023, San Diego, CA and Online
AIAA AVIATION 2023 Forum

10.2514/6.2023-4118

Effect of Horizontal and Vertical Overlap on the performance of two-bladed Vertical Axis Wind turbine

Rithik R. Nambiar[1] Manish Tripathi[2] Rajkumar S. Pant[3]
Indian Institute of Technology Bombay, Mumbai, Maharashtra, 400076, India

Harnessing wind energy is one of the cleanest forms and abundantly available to generate electricity. Wind turbines produce electricity from the wind power to drive the electric generators. There are two types of Wind turbines depending on the axis of rotation with the respect to the ground, Horizontal axis wind turbines (HAWT) and Vertical axis wind turbines (VAWT). In urban areas, due to the space compatibility and skewed wind conditions, VAWT are preferred. There are two types of VAWT, lift-type configuration like Darrieus wind turbine and drag-type configuration like Savonius wind turbines. Due to factors like self-starting capabilities and better performance even in low-speed winds, Savonius wind turbines are preferred. The present paper, Effect of Overlap Ratio on the blade performance are investigated and analysed. For this, the diameter of the rotor is maintained. Two dimensional numerical simulations are performed using RANS equations and sliding-mesh method. The turbulence model employed is SST k- ω model. Change in the RPM due to overlap distance at various inlet wind speeds were analysed and compared. The performance of zero overlap ratio and optimal mode at overall overlap ratios are compared.

Nomenclature

C_p	=	Power coefficient
D	=	Diameter of the rotor
d	=	Diameter of the blade
e	=	overlap distance
ε	=	Kinetic energy dissipation
k	=	Turbulence Kinetic Energy
ω	=	Specific Dissipation rate
V	=	Inlet wind velocity

I.Introduction

The increasing energy needs and the reduction in fossil fuel resources, as well as the environment and global warming strict laws, attract more industries and government agencies towards renewable energy sources [1–3]. The 2015 reports on global energy say that the use of nuclear, fossil, and renewable sources is 2.3%, 78.4%, and 19.3%, respectively [4]. Renewable energy includes wind, solar, geothermal, marine, biomass, and hydropower energy, which seems to be the best alternative to humankind's growing energy consumption and replacement of non-renewable resources [5]. Among others, wind energy is considered the cheap source of available renewable energy and is advancing quickly. The capacity to generate power from wind energy has significantly grown to be one of the foremost renewable sources of energy since 1996. The giants of this route are developed countries such as China, the United

[1]Project Research Assistant, Department of Aerospace Engineering, IIT Bombay
[2] Post-Doctoral Fellow, Department of Aerospace Engineering, IIT Bombay
[3] Professor, Department of Aerospace Engineering, IIT Bombay

States, and Germany. The total capacity of wind energy by the end of 2016 was about 487 GW and is expected to be about 2000 gigawatts by 2030.

Wind turbines can be classified in a first approximation according to their rotor configuration of the axes and the type of aerodynamic forces from which wind energy is taken. There are several other features such as rated power, dimensions, number of blades, power management, etc., which can also be used to classify turbines into more specific categories. The two main categories which are based on their axis along which the turbine rotates are HAWT (Horizontal Axis Wind Turbines) and VAWT (Vertical Axis Wind Turbines). Generally, most wind turbines in the market are the Horizontal axis turbines due to their high efficiency in wind power extraction (Figure 1)

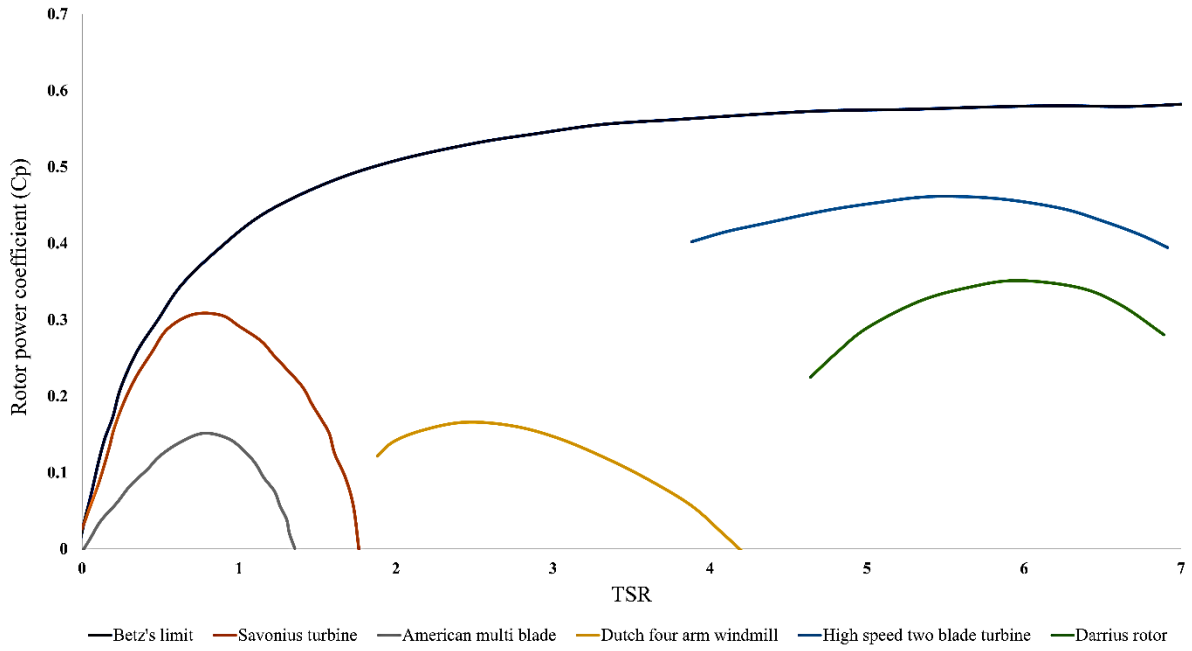

Fig 1. Curve of the rotor power coefficient (Cp) v/s Tip speed ratio (TSR) for different type of wind turbines [6]

In some cases, we can find vertical axis turbines better over horizontal axis turbines like they work independent to wind direction, less noisy which makes them socially acceptable, easy for maintenance, simple construction and cheaper than horizontal axis turbines. Significant developments and benefits of VAWT have been presented by manufacturers and researchers for VAWT [7]. They are suitable for small-scale applications with minimum electrical load as they have better performance under disordered wind conditions due to obstacles like buildings, terrains etc. VAWT tare of two types, lift type-turbines (Darrieus) and drag-type (Savonius). Lift-type turbines are high torque and low-speed turbines which requires external or manual forces to start working. Drag-type are low torque and high-speed turbines with self-start capabilities. In matters of cost efficient and reliability, the latter turbines are suited best for turbulent conditions.

This present work conducts a numerical study of the drag-type conventional semi-circular savonius vertical axis wind turbine. According to the required accuracy, various turbulence models such as RANS, LES, and DNS are used in the simulations. The best accuracy is expected from DNS model but requires higher computational cost [8]. We have used RANS for the present work. A turbulent and transient airflow nature is present around the turbines. Various studies have been performed in recent years to improve their performance. In 2015, Frederikus et al. [9] studied the effect of several blades on the efficiency of the savonius turbine using numerical method. It said that a three-blade wind turbine produces higher rotational speed and tip speed ratio than the two and four blade models. Ebrahimpour et al [10] worked on a numerical study to discern the effect of overlap parameters for two blades using URANS and realizable k-ε model. Improvement percentage of torque coefficient was by 11.5% for horizontal overlap and 16% for vertical overlap.

Improvement percentage of power coefficient was by 3.7% in horizontal overlap and 7.5% in vertical overlap. Muller et al [11] experimentally found that leaving a gap between blades is important and with minimum torque applied, blade velocities can increase up to 2.5 times the wind speed. Roy and Saha et al [12] performed 2D simulations using K-ε under the influence of wall function to find overlap ratios for savonius wind turbines. They concluded that these turbines have high efficiency at the overlap ratio of 0.2. Mohammed et al [13] compared different turbulence model such as SST k- ω, RSM, standard k-ε, and realizable k-ε for a two-dimensional simulation to optimize the conventional savonius turbines. It says that realizable k-ε gave minimum errors compared to experimental data by Hayashi's [14]. From the literature study, we can see that performance can change with geometry modifications like number of blades, rotor height, rotor diameter, wind speed and many other factors. However, the effect of overlap ratios on both the directions hasn't come to knowledge for most of the authors. The difference in this study is negative and positive overlapping will be studied on both the axes. Fujisawa et al [15] studies show better torque and rotor power at an overlap ratio of 0.15 when performed on four rotors with overlap ratios between 0 to 0.5.

The present study explains about Overlap ratio in horizontal and vertical axes and analyse the change in performance by RPM Output. For this, one of the blades will be placed geometrically as a reference. First, it will be displaced along the X-axis to find an optimal point. From the X axis optimal point, the blade will be displaced along the Y axis to reach the final optimal point. The change in RPM due to overlap distance will be evaluated for this study.

II.Numerical Methodology

The savonius wind turbine works as a simple turbine because of the drag difference between rotors. The wind filled in concave part absorbs the air and induces the blades to rotate, while the convex part counters the rotation. When moving towards the wind, difference in drag force enables the blades to rotate as shown in Figure 2 [17]

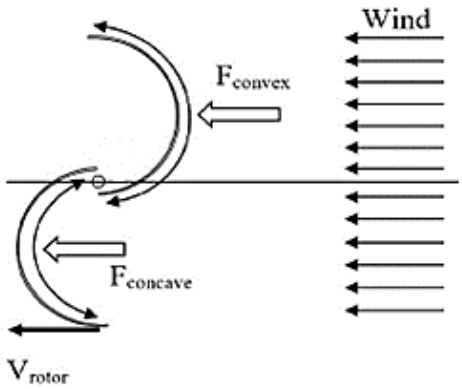

Fig 2. Two blade savonius wind turbine rotating due to the drag difference [18]

A. Note on Overlap Ratio

The region between two blades is called overlap distance. The difference in concave and convex sides in pressure can be compensated. The definition and formula for overlap ratio has been explained differently in different studies. Roy and Saha et al [16] explained the general overlap ratio to be:

$$Overlap\ ratio = e/d$$

Where, e is the overlap distance between the blades, d is the diameter of the blade and D is the diameter of the turbine (Figure 3). In our study we are looking at overlap distances in both the X and Y direction. To do this for a three-blade rotor, we must take one blade as a reference with the bottom tip as the reference point (RP). The position of this RP will be changed in Y axis initially and then in X axis.

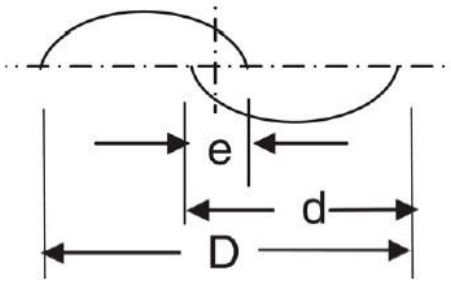

Fig 3. Diagram of overlap ratio [16]

The process of getting an optimal overlap is follows: first the reference blade is translated along Y direction which makes the RP coordinates to be (0, y) where (0, B) will be the optimal constant point. Now, RP will be translated in X axis whose coordinates will be (x, B) where (A, B) will be the optimal point. Thus, best position of the blades can be found if the sweep area is kept constant. So, from Ebrahimpour et al [10] defined overlap ratio as:

$$\textit{Horizontal overlap ratio (HOLR)} = e_1/d$$
$$\textit{Vertical overlap ratio (VOLR)} = e_2/d$$

Depending on the position of RP, the HOLR and VOLR can be positive and negative. HOLR values will be negative if the HOLR is in the negative side of the X axis. For VOLR to be negative, the RP should be moving away from the Y axis (Figure 4). If there is overlap, the ratios are positive; otherwise, they are negative.

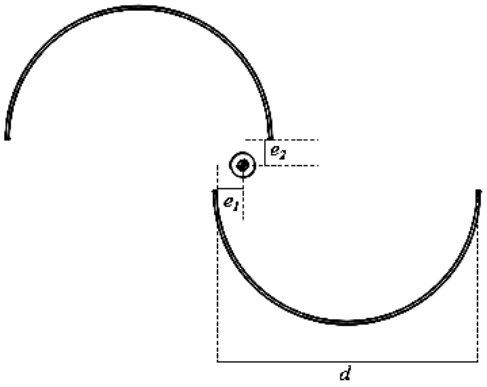

Fig 4. Schematic diagram of overlap ratio separated defined for horizontal and vertical distance

Our study is based on a light weight VAWT which has dimensions and specifications as given in Table 1. The wind speeds considered for the simulations are considered from the data from Global wind atlas in India [22]. For an average altitude of 50m in 2022, Wind speeds between 4m/s to 9m/s are considered. In the present work, wind velocities of 5 m/s, 6 m/s and 7m/s are chosen.

Table 1. Blade specifications of the VAWT used for the simulations

Blade diameter	0.4 m
Blade thickness	0.005 m
Blade height	1 m
Blade material	Fibre reinforced polymer
Density of the material	1522 Kg/m^3
Weight of the blades	9.683 Kg

Simulation was done initially for horizontal overlap ratios. The overlaps of 0, +0.05, +0.1, +0.15, +0.2, +0.25, -0.1, -0.2 are investigated to find the best possible ratio (Figure 5) and hence calculate the RPM and TSR. Revolutions per minute (RPM) which for a VAWT is expressed as:

$$\text{RPM} = \frac{60 * V * TSR}{\pi * D}$$

Tip speed ratio (TSR) is the ratio of blade tip speed and inlet wind velocity as follows:

$$\text{TSR} = \lambda = \frac{Vrotor}{V} = \frac{\omega * d}{V}$$

V_{rotor} is the rotor tip velocity (m/s); ω is the rotational speed (rad/s)

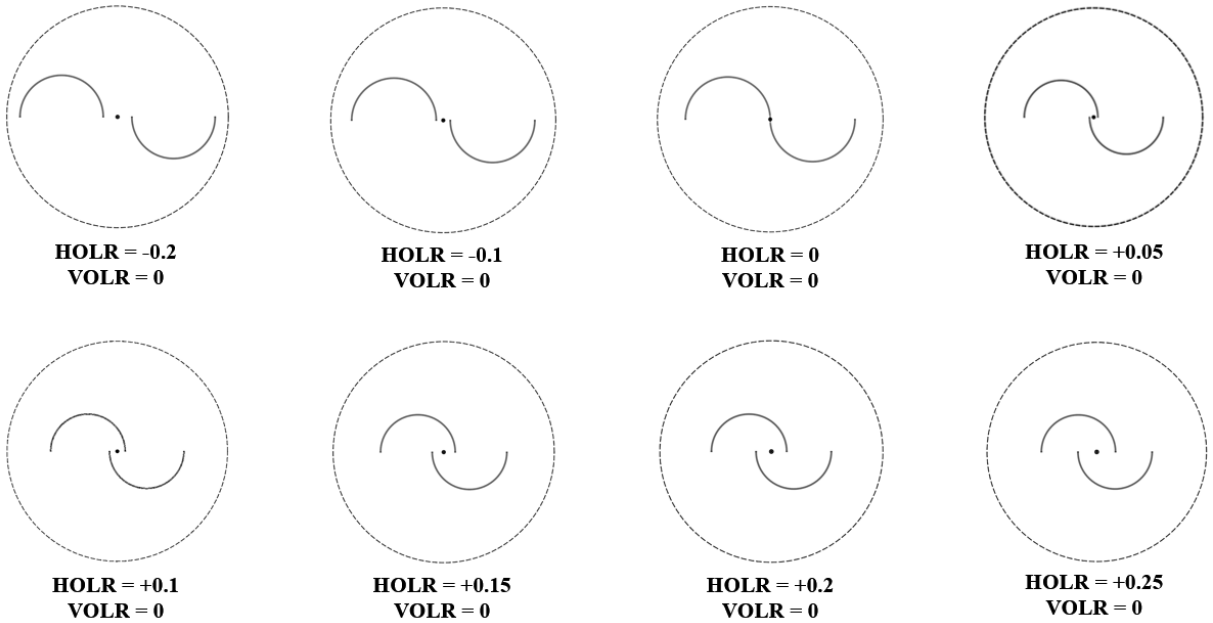

Fig 5. 2D drawings of rotors with horizontal overlap ratios

B. Governing equations

For numerical analysis of present study, Reynolds-averaged Navier Stoker (RANS) equations are used. An outline of the numerical solutions involved, and the mathematical models are as follows [23]:

Continuity of mass:

$$\frac{\partial \rho}{\partial t} + \frac{\partial}{\partial x_j}[\rho u_j] = 0$$

Equations of motion:

$$\frac{\partial}{\partial t}[\rho u_i] + \frac{\partial}{\partial x_j}[\rho u_i u_j + p\delta_{ij} - \tau_{ji}] = 0, \quad i = 1,2,3$$

Conservation of energy:

$$\frac{\partial}{\partial t}[\rho e_0] + \frac{\partial}{\partial x_j}[\rho u_j e_0 + u_j p + q_j - u_i \tau_{ij}] = 0$$

Here, t is the time, x_j is the j[th] component of the position vector, u_j is the j[th] component of the velocity vector, p is the pressure, ρ is the density, $\delta_{ij} = 1$ for $i = j$ and zero. τ_{ji} is the viscous shear stress, e_0 is the total energy, and q_j is the heat flux.

C. Computational Domain

The computational domain was divided into two domains as shown in Figure 6 so that the rotor can be rotated. The best and smaller grid size is for the rotor components. The outer domain or stationary domain has lower resolution of cells compared to the rotating domain. The whole computation domain has the dimensions 15 m x 8 m. The inlet distance from the centre of the rotor is 3m. The diameter of the rotating zone is three times the diameter of the blade which is 1.2 m. Eliminate the effect of the domain walls, the dimensions of the domain were made broad enough.

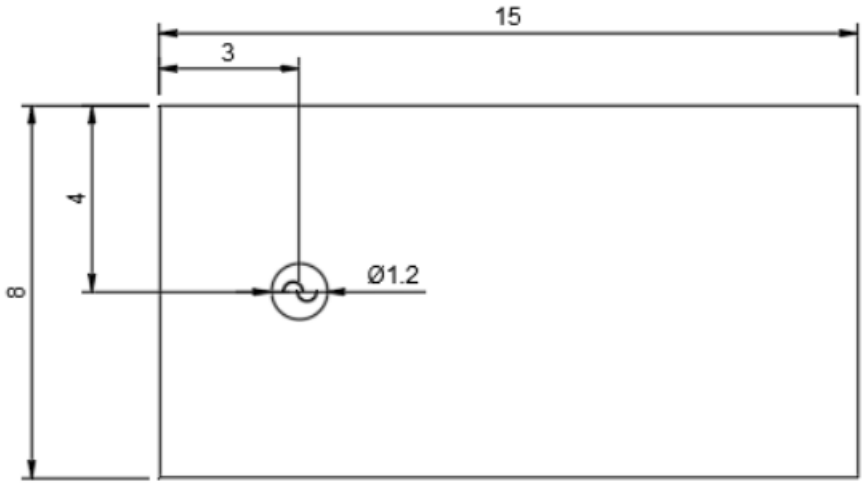

Fig 6. Computational Domain with Dimensions (in meters)

D. Mesh setup and Boundary Conditions

Sliding mesh is used to mesh the unstable flow area of the solution [21]. The relative motion between the stationary and moving domain is measured using this method. Different cell dimensions are used to preserve mesh consistency in the computational domain. Majority of the domain is implemented with triangular meshes. The wall of the blades was refined using quadrilateral meshes to achieve better performance. Mesh quality smoothing is set to high. Around the rotor, inflation mesh of 10 layers is implemented to consider the effects of the wall. The cell size implemented in different areas and inflation is shown in Figure 7. Interface between the rotating and stationary domain was established.

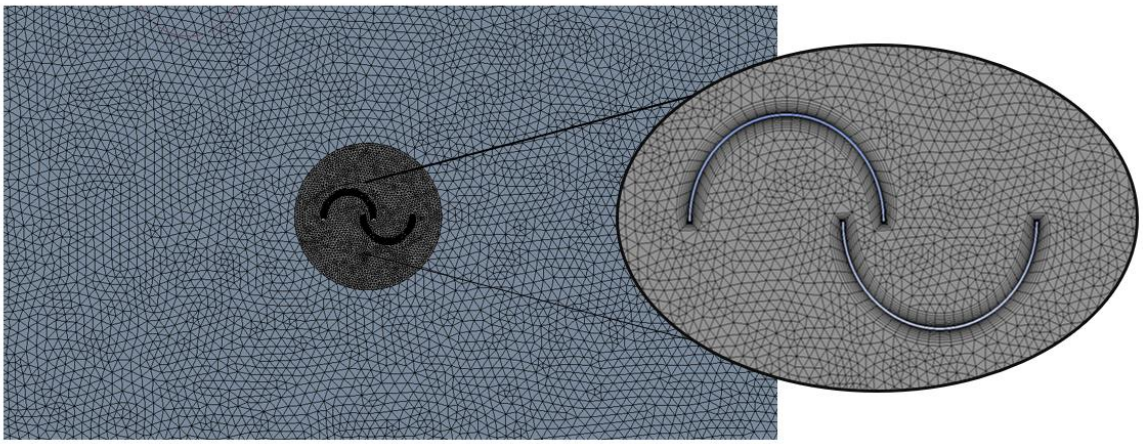

Fig 7. Triangular mesh with 10 layers of inflation for a rotor with HOLR = +0.1 and VOLR =0

Free stream uniform inlet was chosen on the left side of the computational domain. The gauge pressure is 0 Pa, the turbulence strength is 5% and the viscosity ratio is 10. The pressure-outlet boundary is on the right side of the computational domain with an absolute pressure of 0 Pa. Symmetry boundary conditions are extended on the top and bottom. Adjoining rotary mesh is the interfaces present onto the stationary outer domain.

III. Results and Discussion

E. Grid Independence

To investigate the mesh independence, the element size is changed from 45000 to 140000 (Figure 8). From the study, the results show that as the number of cells increased from 50000, the steady state velocity curve relative to the number of cells reaches approximately zero. Therefore, grid with 50000 cells was appropriate for the study.

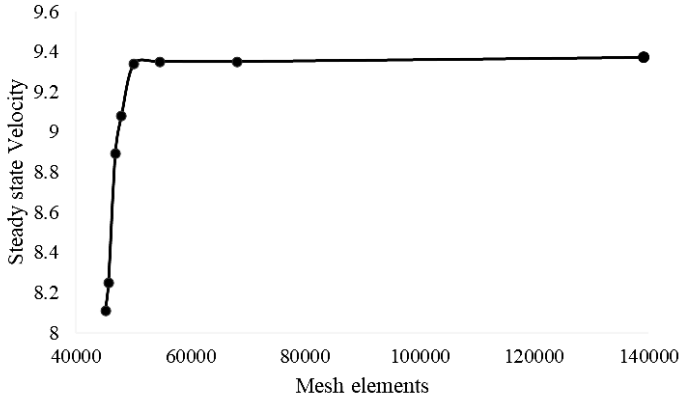

Fig 8. Mesh Independence study done from 45000 to 140000 cells

F. Effect of HOLR on RPM of the VAWT

Keeping the VOLR zero, The HOLR was analysed, the RPM curve relative to the HOLR was obtained for 5 m/s, 6 m/s and 7m/s as in Figure 10. At HOLR of +0.1, maximum RPM obtained with the value of 255 at 7 m/s, 220 at 6 m/s and 184 at 5 m/s compared to HOLR of 0 which had values of 248 at 7 m/s, 214 at 6 m/s and 178 at 5 m/s.

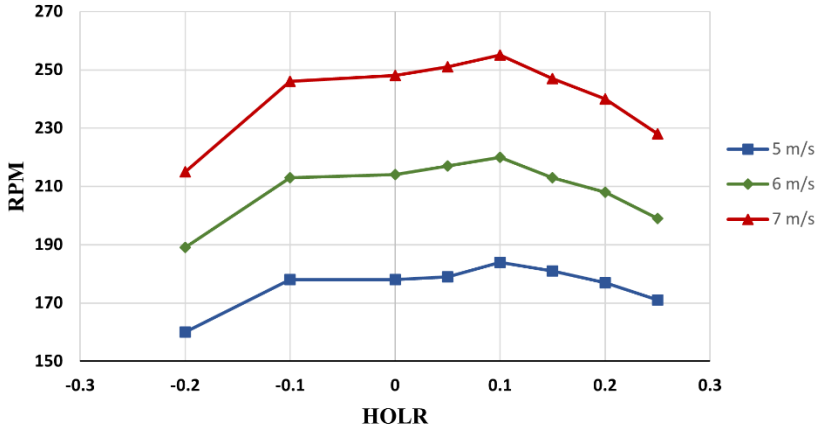

Fig 9. RPM obtained at different Horizontal Overlaps with Vertical Overlap (VOLR) of zero

G. Effect of VOLR on RPM of the VAWT

After deciding the horizontal overlap ratio point, i.e., HOLR =+0.1, variations of the vertical overlap ratios are studied as shown in Figure 10. For this, primarily the overlaps of -0.15, -0.1, -0.05, +0.05, +0.1, +0.15 are investigated to find the best possible ratio and calculate the RPM.

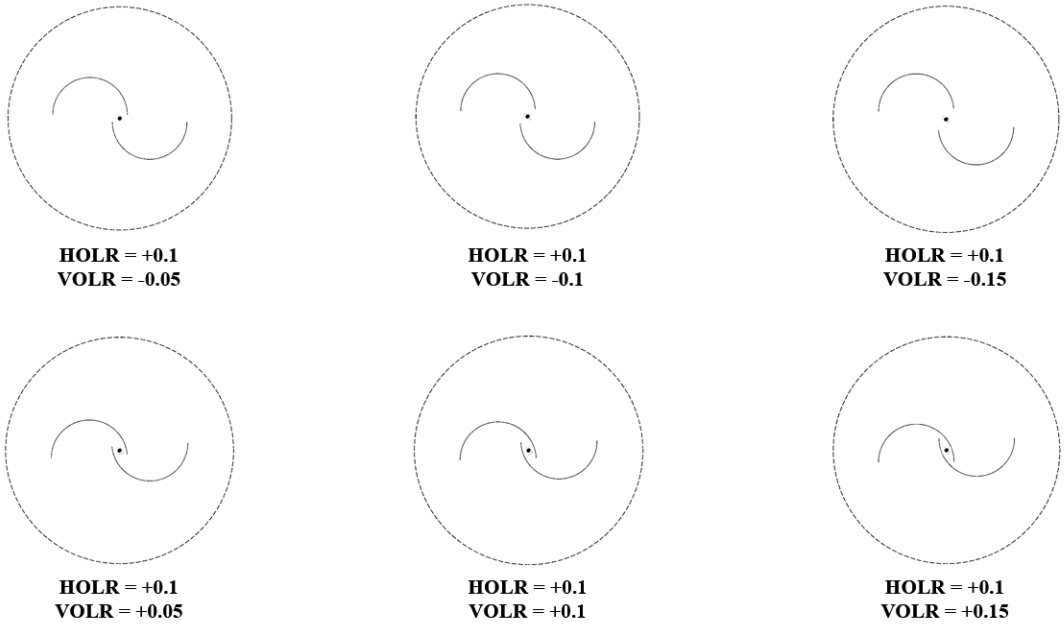

Fig 10. 2D drawings of rotors with vertical overlap ratios

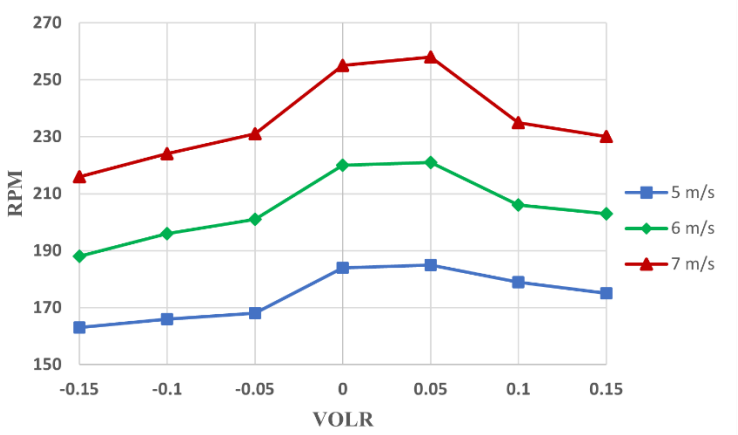

Fig 11. RPM obtained at different Vertical Overlaps with HOLR = +0.1

Based on maintaining HOLR at an optimal level of +0.1, it can be observed from Figure 11 that when VOLR is set to +0.05 at velocities of 5 m/s, 6 m/s, and 7 m/s, the resulting RPM values are 185, 221, and 258, respectively. While an improvement in RPM can be noted at VOLR = +0.05 during optimization, the increase is comparatively lower than that achieved through HOLR optimization. Table 2 shows the percentage change of RPM at HOLR = +0.1 with reference to the value obtained at the origin and Overall Overlap ratio with reference to the origin. The average increase about the HOLR optimization and Overall Overlap ratio comes out to be around 3% and 3.7% respectively.

Table 2. Comparison of the RPM value at zero overlap ratio and optimal Horizontal and Vertical overlap ratio

Inlet Wind velocity	RPM HOLR = 0 VOLR = 0	RPM HOLR = +0.1 VOLR = 0	RPM HOLR = +0.1 VOLR=+0.05	% Increase about Optimization of Horizontal Overlap ratio	% Increase about Optimization of Overall Overlap ratio
5 m/s	178	184	185	3.37	3.93
6 m/s	214	220	221	2.80	3.27
7 m/s	248	255	258	2.82	4.03

The basis of the change in performance is due to the presence of the overlap distance and the return flow from the front concave blade to the convex blade at the back. This reduces the negative pressure created on the convex blade due to the inlet wind. This is due to the tendency of the fluid to be attached on the convex surface on the concave section of the blade i.e., Coanda flow. At negative overlap ratios, due to the absence of the return flow, lower values of RPM are obtained. Figure 12 and Figure 13 shows the velocity contour of the VAWT at the optimal Horizonal and Overall overlap ratio respectively.

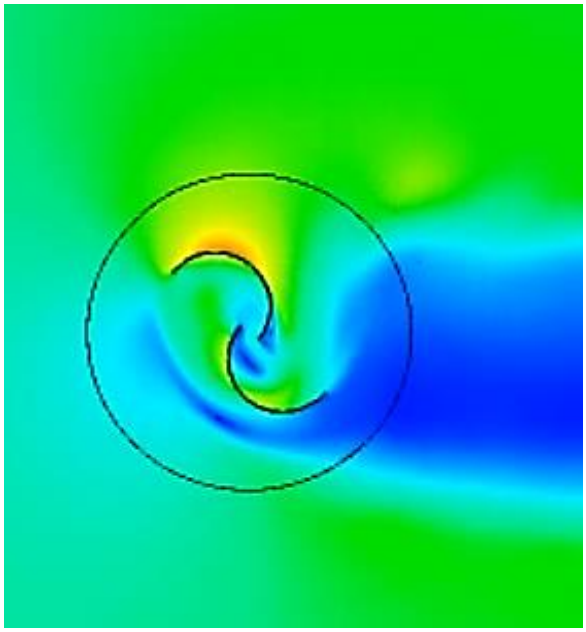

Fig 12. Velocity contour of the VAWT at HOLR= +0.01 and VOLR =0

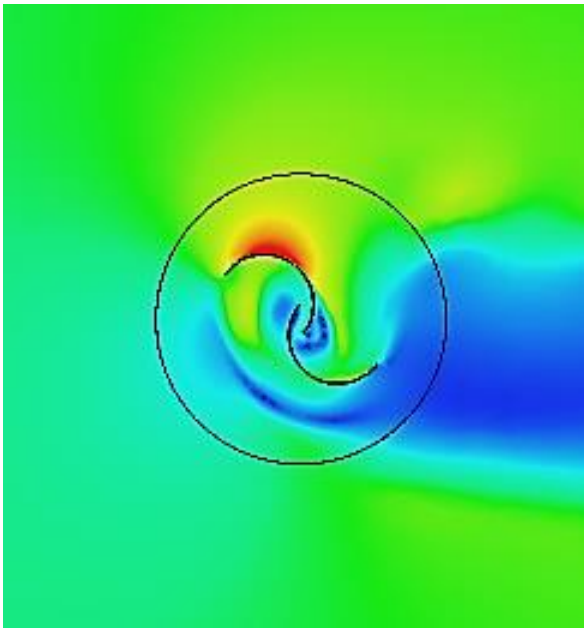

Fig 13. Velocity contour of the VAWT at HOLR= +0.1 and VOLR = + 0.05

IV. Conclusion

This research analyses the performance of a Savonius wind turbine by maintaining a constant blade diameter and varying the overlap ratios in the horizontal and vertical directions. The study employs Computational Fluid Dynamics (CFD) using RANS equations and the SST K-ω turbulence model to conduct simulations. The findings indicate that better performance is achieved at near zero and positive horizontal and vertical overlap ratios as compared to other states. The rotor with HOLR = + 0.1 demonstrates a higher rpm at various inlet wind speeds, thus considered as the optimal overlap in this study. Subsequently, the study examines the vertical overlaps at this optimal point. The results suggest that VOLR = +0.05 produces better performance compared to other overlaps. Therefore, HOLR = +0.1 and VOLR = +0.05 are considered as the optimal overall overlap ratio. When considering the same base state, the average improvement percentage of horizontal overlap is around 3%, and the overall overlap is 3.7%

V.References

[1] Alamian, R.; Shafaghat, R.; Miri, S.J.; Yazdanshenas, N.; Shakeri, M. Evaluation of technologies for harvesting wave energy in Caspian Sea. Renew. Sustain. Energy Rev. 2014, 32, 468–476.

[2] Ghasemian, M.; Ashrafi, Z.N.; Sedaghat, A. A review on computational fluid dynamic simulation techniques for Darrieus vertical axis wind turbines. Energy Convers. Manag. 2017, 149, 87–100.

[3] Roy, S.; Ducoin, A. Unsteady analysis on the instantaneous forces and moment arms acting on a novel Savonius-style wind turbine. Energy Convers. Manag. 2016, 121, 281–296.

[4] Sawin, J.L.; Sverrisson, F.; Seyboth, K.; Adib, R.; Murdock, H.E.; Lins, C.; Appavou, F.; Brown, A.; Chernyakhovskiy, I.; Epp, B.; et al. Renewables 2017 Global Status Report; REN21: Paris, France, 2013.

[5] Mohammadi, M.; Lakestani, M.; Mohamed, M. Intelligent parameter optimization of Savonius rotor using artificial neural network and genetic algorithm. Energy 2018, 143, 56–68.

[6] Ajayi, O. Application of Automotive Alternators in Small Wind Turbines. Master's Thesis, Delft University of Technology, Delft, Netherlands, 2012.

[7] Svorcan, J.; Stupar, S.; Komarov, D.; Pekovi´c, O.; Kosti´c, I. Aerodynamic design, and analysis of a small-scale vertical axis wind turbine. J. Mech. Sci. Technol. 2013, 27, 2367–2373.

[8] Ducoin, A.; Shadloo, M.; Roy, S. Direct numerical simulation of flow instabilities over Savonius style wind turbine blades. Renew. Energy 2017, 105, 374–385.

[9] Wenehenubun, Frederikus; Saputra, Andy; Sutanto, Hadi (2015). An Experimental Study on the Performance of Savonius Wind Turbines Related with The Number of Blades. Energy Procedia, 68(), 297–304. doi: 10.1016/j.egypro.2015.03.259

[10] Ebrahimpour, Mohammad; Shafaghat, Rouzbeh; Alamian, Rezvan; Safdari Shadloo, Mostafa (2019). Numerical Investigation of the Savonius Vertical Axis Wind Turbine and Evaluation of the Effect of the Overlap Parameter in Both Horizontal and Vertical Directions on Its Performance. Symmetry, 11(6), 821
[11] Müller, G.; Chavushoglu, M.; Kerri, M.; Tsuzaki, T. A resistance type vertical axis wind turbine for building integration. Renew. Energy 2017, 111, 803–814.
[12] Roy, S.; Saha, U.K. Computational study to assess the influence of overlap ratio on static torque characteristics of a vertical axis wind turbine. Procedia Eng. 2013, 51, 694–702.
[13] Mohamed, M.; Janiga, G.; Pap, E.; Thévenin, D. Optimal blade shape of a modified Savonius turbine using an obstacle shielding the returning blade. Energy Convers. Manag. 2011, 52, 236–242.
[14] Hayashi, T.; Li, Y.; Hara, Y. Wind tunnel tests on a different phase three-stage Savonius rotor. JSME Int. J. Ser.B Fluids Therm. Eng. 2005, 48, 9–16.
[15] Fujisawa, N. On the torque mechanism of Savonius rotors. J. Wind Eng. Ind. Aerodyn. 1992, 40, 277–292.
[16] Roy, S.; Saha, U.K. Review of experimental investigations into the design, performance, and optimization of the Savonius rotor. Proceedings of the Institution of mechanical engineers, part A. J. Power Energy 2013, 227,528–542.
[17] Abdul Akbar, M.; Mustafa, V. (2016). A new approach for optimization of Vertical Axis Wind Turbines. Journal of Wind Engineering and Industrial Aerodynamics, 153(), 34–45. doi: 10.1016/j.jweia.2016.03.006
[18] M.H. Pranta; M.S. Rabbi;M.M. Roshid; (2021). A computational study on the aerodynamic performance of modified savonius wind turbine. Results in Engineering, doi: 10.1016/j.rineng.2021.100237
[19] H. Gad, M.H. Nasef, A New Design of Savonius Wind Turbine: Numerical Study,2014.
[20] M. Lundberg, A. Manousidou, J. Solhed, J. Sundberg, Two-dimensional Study of Blade Profiles for a Savonius Wind Turbine, 2020
[21] I. Hashem, M.H. Mohamed, Aerodynamic Performance Enhancements of H-Rotor Darrieus Wind Turbine, Elsevier B.V., 2017.
[22] Global wind atlas. Available online: https://globalwindatlas.info/en/area/India (Accessed on 26 October 2022)
[23] Cai, J., "Numerical Study on Choked Flow over Grid-Fin Configurations," Journal of Spacecraft and Rockets, Vol. 46, No. 5, 2009, pp. 949–956.